# Pairwise Interaction Point Processes for Modelling Bivariate Spatial Point Patterns in the Presence of Interaction Uncertainty

Journal of Environmental Statistics

September 2015, Volume 7, Issue 3. http://www.jenvstat.org

# Pairwise Interaction Point Processes for Modelling Bivariate Spatial Point Patterns in the Presence of Interaction Uncertainty

**Glenna F. Nightingale** [1], **Janine B. Illian** [2], **and Ruth King** [3]
*glenna.evans@gmail.com, janine@mcs.st-and.ac.uk, Ruth.King@ed.ac.uk*
[1]School of Geography and Geosciences
[2]School of Maths & Statistics and Centre for Ecology and Envrionmental Research
University of St. Andrews, Scotland, KY16 9LZ, U.K.
[3]School of Mathematics, University of Edinburgh,
James Clerk Maxwell Building, The Kings Buildings, Peter Guthrie Tait Road,
Edinburgh, EH9 3FD, U.K.

**Abstract**

Current ecological research seeks to understand the mechanisms that sustain biodiversity and allow a large number of species to coexist. Coexistence concerns inter-individual interactions. Consequently, there is an interest in identifying and quantifying interactions within and between species as reflected in the spatial pattern formed by the individuals. This study analyses the spatial pattern formed by the locations of plants in a community with high biodiversity from Western Australia. We fit a pairwise interaction Gibbs marked point process to the data using a Bayesian approach and quantify the inhibitory interactions within and between the two species. We quantitively discriminate between competing models corresponding to different inter-specific and intraspecific interactions via posterior model probabilities. The analysis provides evidence that the intraspecific interactions for the two species of the genus *Banksia* are generally similar to those between the two species providing some evidence for mechanisms that sustain biodiversity.

Keywords: Gibbs point processes; Multivariate spatial point patterns; Reversible jump Markov chain Monte Carlo.

# 1. Introduction

## 1.1. Modelling Biodiverse Plant Communities

Mechanisms or biological processes which maintain biodiversity and hence facilitate the coexistence of a large number of species have been the focus of numerous ecological studies (Grinnell 1917; Janzen 1970; Hubbell 1997; Siepielski and McPeek 2002; Wright 2002; Murrell and Law 2003; Zillio and Condit 2007). Consequently, an understanding of such processes is of central importance to biodiveristy preservation.

Modelling species interactions in a spatial context involves analysing the spatial pattern formed by individuals in ecological communities to reveal the individuals' local interactions and hence to inform on the interaction structure in a community (Murrell and Law 2003). A spatial point pattern therefore can be considered as a spatial signature, which, if decoded, can shed light on the interactions among and within the species in a plant community. A growing number of publications has focused on the analysis of these spatial point patterns both based on descriptive statistics (Liebhold and Gurevitch 2002; Wiegand and Moloney 2004; Comas and Mateu 2007) and on point process models (Thompson 1955; Gatrell *et al.* 1996; Khaemba 2001).

Spatial point process models describe the overall properties of spatial patterns, while taking every individual in a community into account (Illian et al. 2008). Both in the ecological and in the statistical literature, most studies using spatial point processes, model the pattern formed by a single species only (Illian *et al.* 2012; Ewel and Hiremath 2006; Møller and Waagepetersen 2003; Diggle 2003; Callaway 1995). So far, few studies involve multivariate patterns i.e. patterns formed by two or more species (Baddeley and Turner 2000; Wiegand *et al.* 2007; Illian *et al.* 2009; Picard *et al.* 2009). However, in models of multi-species patterns the number of "intra-", and "inter-" specific interactions and hence the number of interaction parameters grows with the number of species. Hence suitable methods for model selection are required to compare different models and to avoid over-parameterization. In this analysis we consider a two species (bivariate) dataset comprising of species of the same genus.

## 1.2. The Dataset

The dataset comprises of two species of the genus *Banksia*, from a $22 \times 22$ metre plot from Cataby, Western Australia (Armstrong 1991). The two species have been classified as resprouters, which exhibit a particular fire regeneration strategy. Resprouters regenerate from root stocks after a fire (Bell 2001). Due to low nutrient levels in the sandy soil that characterize the study area, resprouters reproduce very slowly but the existing individual plants are likely to have existed in the same location for a very long time (Armstrong 1991; Illian *et al.* 2009). Overall, environmental conditions, in particular the nutrient and water levels in the soil may be considered homogeneous within the plot (Armstrong 1991; Illian *et al.* 2009). As a result of the homogeneity of the soil conditions, this dataset allows us to model interactions within a plant community without the need to include environmental spatially explicit covariates that potentially impact on the pattern.

To illustrate the proposed approach, we consider the spatial pattern formed by two resprouter species, *Banksia menziesii* and *Banksia attenuata*. We develop a Bayesian approach to fitting spatial point processes models, in particular Gibbs processes, and consider reversible jump

methods to discriminate between competing models in terms of the interactions present within and between species (or intra- and inter-specific interactions respectively). Figure 1 illustrates the bivariate point pattern formed by the two resprouter species in this study.

[Figure 1 about here.]

### 1.3. Exploratory analysis

An exploratory analysis of the data was conducted using the L-function Besag (1977) and the pair correlation function (Diggle 1983; Baddeley *et al.* 2007; Stoyan and Penttinen 2000; Illian *et al.* 2008; Law *et al.* 2009) .

*L-function*

The L-function was introduced by Besag (1977), and is strongly related to Ripley's K function. This function is commonly expressed as $L(r)$, where $r$ denotes the interaction radius, may be used to assess point patterns for complete spatial randomness. Typically, the empirical L-function is compared to that obtained for a point pattern derived from Poisson point process (theoretical L-function). The value of the theoretical L-function is equal to $r$ for a stationary Poisson process at all distances. In this analysis, the L-function was plotted for each species, each with a corresponding simulation envelope obtained from 10,000 instances (Figure 2) of a Poisson point process.

[Figure 2 about here.]

In each plot, the theoretical L-function is denoted by a dotted red line and the empirical L-function by a solid black curve. If the curve obtained for the empirical L-function was above/below the simulation envelope, this could indicate the possibility of clustering/regularity beyond that expected under conditions of complete spatial randomness (CSR). The inclusion of simulation envelopes around the line for the theoretical L-function gives us an indication of how much deviation is associated with the realisations.

In general, the curve for the empirical L-function for *Banksia menziesii* fluctuates above and below the reference line representing the theoretical L-function. Despite this, the curve remains within the simulation envelopes. For *Banksia attenuata*, the curve for the empirical L-function is observed to be predominantly above the line representing the theoretical L-function, this however remains within the simulation envelopes. Overall, we note that both plots fall within the respective simulation envelopes thus providing no evidence against complete spatial randomness at the exploratory level.

*Pair correlation function*

The pair correlation function, commonly expressed as *g(r)*, is also useful in providing a spatial summary of a given point pattern. Specifically, *g(r)* provides an indication of the dependency of points at a given distance $r$ for a given point pattern. This function is a derivative of Ripley's K function and is expressed as

$$g(r) = \frac{K'(r)}{2\pi r} \forall r \geq 0.$$

For point pattern which exhibits CSR, $g(r) = 1$ for all values of $r$. If $g(r) > r$ this suggests that there is spatial dependency between the points. That is, the interpoint distance $r$ occurs more frequently than under conditions of CSR. The converse is true for $g(r) < 1$. If $g(r) = 0$, this suggests that there are no points within the specified interpoint distance $r$. In this case $r$ is termed a 'hard core radius'. The pair correlation function was plotted for both species and is shown in Figure 3 with simulation envelopes obtained from 10,000 replications of a Poisson point process.

[Figure 3 about here.]

From Figure 3 it is clear that for each species, the corresponding empirical plot fluctuates above and below the reference line, but remains within the simulation envelopes. This suggests that there is no evidence against CSR.

These summary characteristics only provide preliminary results and are limited in that each analysis only assess the behaviour of a single species in the study area. A more formal approach would include point process models which provide estimates of the interactions between species. We focus on these models in the next section.

# 2. Method

## 2.1. Gibbs processes, specific model choice

Gibbs processes are point processes which model patterns exhibiting inhibition or aggregation, i.e. interaction among the points (Illian *et al.* 2008). We consider a pairwise-interaction Gibbs process (Baddeley and Turner 2000) to model a bivariate point pattern. In particular, we let the points in a given point pattern $\boldsymbol{x}$, contained in a bounded region in space $W$, represent objects of interest such as plants. If each point is accompanied by additional information (such as which species it represents) the point pattern is a marked point pattern (Illian *et al.* 2008). Each point is associated with a mark $m \in M$ where $M$ is the mark space. In our example we let the marks denote the different species of interest so that $M = \{1, 2\}$.

A Gibbs process is characterized by a set of intensity and interaction parameters. The intensity parameters, are denoted by $\beta_1$ and $\beta_2$ and represent the intensity of plants per unit area ($1dm^2$) from species 1 and species 2, respectively. The full parameter set for the Gibbs process used here is denoted by $\boldsymbol{\theta} = \{\beta_1, \beta_2, \gamma_{11}, \gamma_{22}, \gamma_{12}\}$.

In general, pairwise interaction processes are suitable for modelling regular point patterns, whereas area interaction point processes are appropriate for modelling aggregated point patterns (King *et al.* 2012). In the pairwise interaction process we consider here, interactions within or between species groups are negative interactions and are inhibitory in nature. The interaction parameters take values within the range of 0 to 1 where lower values indicate a higher degree of inhibition. In the special case where the interaction parameter is 0 there is hard core inhibition such that there is a circle of fixed interaction radius around each plant within which no other plant is found. Conversely, an interaction parameter of 1 corresponds to no interaction resulting in complete spatial randomness.

Let $n_1$ and $n_2$ denote the number of individuals in species 1 and 2 respectively, and set $\boldsymbol{v_1} = \{v_{11}, \ldots, v_{1n_1}\}$ and $\boldsymbol{v_2} = \{v_{21}, \ldots, v_{2n_2}\}$ where $v_{ij}$ denotes the $j^{th}$ point for species $i$.

For notational convenience the full set of data is denoted by $\boldsymbol{\upsilon} = \{\boldsymbol{\upsilon_1}, \boldsymbol{\upsilon_2}\}$.

To specify the interaction function we follow Illian *et al.* (2009). For the two point patterns $\boldsymbol{\upsilon_1}$ and $\boldsymbol{\upsilon_2}$ we express the interaction function $s(\boldsymbol{\upsilon_1}|\boldsymbol{\upsilon}_2)$ as

$$s(\boldsymbol{\upsilon_1}|\boldsymbol{\upsilon}_2) = \sum_{i=1}^{n_1}\sum_{j=1}^{n_2} h(\|\upsilon_{1i} - \upsilon_{2j}\|), \tag{1}$$

where $\|\upsilon_{1i} - \upsilon_{2j}\|$ represents the Euclidean distance between $\upsilon_{1i}$ and $\upsilon_{2j}$. We express $h$ in the form:

$$h(r) = \begin{cases} (1-(r/R)^2)^2 & \text{if} \quad 0 < r \leq R \\ 0 & \text{otherwise,} \end{cases}$$

where $R$ is a fixed interaction radius as mentioned earlier. We note that for this interaction function, the magnitude of the interaction between plants is not considered to be constant as for example in a Strauss process, but to decrease with increasing distance (up to a fixed distance $R$).

The interaction parameters $\gamma_{11}$, $\gamma_{22}$ and $\gamma_{12}$ represent the interaction within conspecifics of species 1, within conspecifics of species 2 and between individuals from species 1 and 2, respectively.

The corresponding pseudolikelihood of the data can be expressed as a function of the intensity parameters $\boldsymbol{\beta} = \{\beta_1, \beta_2\}$ and the interaction parameters $\boldsymbol{\gamma} = \{\gamma_{11}, \gamma_{22}, \gamma_{12}\}$ (Baddeley and Turner 2000). In particular we have,

$$f(\boldsymbol{\upsilon}; \boldsymbol{\theta}) = \alpha \beta_1^{n_1} \beta_2^{n_2} \gamma_{11}^{s(\boldsymbol{\upsilon_1}|\boldsymbol{\upsilon_1})} \gamma_{22}^{s(\boldsymbol{\upsilon_2}|\boldsymbol{\upsilon_2})} \gamma_{12}^{s(\boldsymbol{\upsilon_1}|\boldsymbol{\upsilon_2}) + s(\boldsymbol{\upsilon_2}|\boldsymbol{\upsilon_1})},$$

where $\alpha$ is an intractable normalising constant given by

$$\alpha = \exp\left(-\beta_1 \int_W \gamma_{11}^{t(u,\boldsymbol{\upsilon}_1)} \gamma_{12}^{t(u,\boldsymbol{\upsilon}_2)} du - \beta_2 \int_W \gamma_{12}^{t(u,\boldsymbol{\upsilon}_1)} \gamma_{22}^{t(u,\boldsymbol{\upsilon}_2)} du\right), \tag{2}$$

for the function $t$ defined below. Let $u$ be an arbitrary point in the study region $W$. For $i = 1, 2$, we set

$$t(u, \boldsymbol{\upsilon_i}) = \sum_{k=1}^{n_i} h(\|u - \upsilon_{ik}\|). \tag{3}$$

An approximation to this integral term can be obtained by using numerical integration techniques such as the Berman-Turner device (Baddeley and Turner 2000). This pseudolikelihood is expressed for the saturated model which contains all the possible interactions $\gamma_{11}, \gamma_{22}$ and $\gamma_{12}$. Submodels can be defined by different combinations of the presence or absence of these three interaction parameters. In total, for a bivariate point pattern, eight different models can be constructed corresponding to the inclusion or exclusion of each of the different interaction terms in the model.

Border edge correction was used in this analysis. Consequently, parameter estimation is based on a 'reduced sample' or subregion of $W$, such that all the points in the subregion are within at least $R$ units from the boundary of $W$. Note that the points which are within $R$ units from the boundary of $W$, or 'edge points', are still considered as possible 'neighbours' of points in the 'reduced sample'. The reduced sample can be expressed as:

$$W_R = \{u \in W : B(u, R) \subset W\}$$

where $B(u, R)$ represents a disc of radius $R$ centered at $u$. $R$ is chosen here to be equivalent in value to the chosen interaction radius.

The application of border edge correction results in estimating the pseudolikelihood described above using a modified interaction function. The interaction function described in Equation 1, is redefined such that $s(\boldsymbol{v_i}|\boldsymbol{v_j})$ is estimated by $s(\boldsymbol{v_i^-}|\boldsymbol{v_j})$ and the integral in Equation 2 is now expressed over $W_R$ instead of $W$. As a result of the renewed specification of the domain for this integral, the function $t$, described in Equation 3 is redefined such that $u \in W_R$ rather than the previous specification of $u \in W$.

Various methods have been proposed for estimating the interaction radius used in point processes when relevant knowledge is not available. The consideration of the radius of interaction as a model parameter has been explored by Illian *et al.* (2008) and Berthelsen and Møller (2002). Illian *et al.* (2008) construct a hierarchical model of one group of species given the spatial location of a second species group. For this analysis a flat prior of $N(0, \sigma^2)$ restricted to $[0, \infty)$ is used for the interaction radii parameters. One challenge identified in this study is that for a highly biodiverse dataset, the high dimensionality of the set of interaction radii results in high computational costs. Alternatively, Berthelsen and Møller (2002) treat the interaction radius as a parameter where spatial birth and death processes are used for perfect simulation of univariate Gibbs point processes.

In other studies the interaction radius is derived from biological knowledge (King *et al.* 2012; Illian and Hendrichsen 2010) and visual inspection of exploratory plots such as the plot of Ripley's K function (Picard *et al.* 2009). King *et al.* (2012) and Illian and Hendrichsen (2010) both model musk-oxen herds using different modelling approaches. Illian and Hendrichsen (2010) and Møller and Waagepetersen (2003) note that the interaction radius may be more formally estimated by using a profile likelihood approach.

For the dataset considered in this paper, the interaction radii specified are based on biological background information provided and cited by Illian *et al.* (2008). A range for the interaction radius for each of the species considered in this analysis is provided. The range for the interaction radius for *B. attenuata* is $1.5 - 4.0$ m and that for *B. menziesii* is $0.5 - 2.5$ m. We adopt an interaction radius of $2.5m$ for each species.

## 2.2. Bayesian Approach

We adopt a Bayesian approach for inference on the model parameters. The joint posterior distribution of the parameters is formed by combining the likelihood of the data with the corresponding prior distribution of the parameters. However, in our case we do not have an explicit likelihood function, but a pseudolikelihood. The use of the pseudolikelihood in a Bayesian context has been proposed by several authors including Efron (1993); Chang and Mukerjee (2006); Ventura *et al.* (2009).

For notational convenience we let the pseudolikelihood of the data given the parameters be denoted as $f(\boldsymbol{v}|\boldsymbol{\theta})$. The posterior distribution of the parameters can be written as:

$$\pi(\boldsymbol{\theta}|\boldsymbol{v}) \quad \propto \quad f(\boldsymbol{v}|\boldsymbol{\theta})p(\boldsymbol{\theta}),$$

where $p(\boldsymbol{\theta})$ denotes the prior on the model parameters. Given the specification of the model (i.e. specific interaction terms present in the model), and the corresponding priors on the parameters we can obtain posterior estimates of interest using a Markov chain Monte Carlo

(MCMC) algorithm. However due to the additional model uncertainty we extend the posterior distribution to incorporate this additional level of uncertainty. In particular, we treat the model itself as a discrete parameter and form the joint posterior distribution over both parameter and model space, given by,

$$\pi(\boldsymbol{\theta}, m|\boldsymbol{\upsilon}) \quad \propto \quad f_m(\boldsymbol{\upsilon}|\boldsymbol{\theta})p(\boldsymbol{\theta}|m)p(m),$$

where $\boldsymbol{\theta}$ defines the set of parameters in model $m$, $f_m(\boldsymbol{\upsilon}|\boldsymbol{\theta})$ represents the pseudolikelihood of the data given model $m$, $p(\boldsymbol{\theta}|m)$ the prior distribution for the parameters in model $m$ and $p(m)$ the prior probability for model $m$.

To explore the posterior distribution and to obtain posterior summary statistics, we use a reversible jump (RJ) MCMC approach (Green 1995). This approach comprises two distinct steps.

*Step 1.* Update the parameters, conditional on the model, using the Metropolis Hastings algorithm.

*Step 2.* Update the model itself using a reversible jump step.

We consider only the second step in detail, since the Metropolis Hastings algorithm used in the first step is a standard random walk Metropolis update (Brooks 1998).

For the reversible jump step suppose that at iteration $k$, the Markov chain is in model $m$ with parameter vector $\boldsymbol{\theta}$ so that the current model state is denoted as $(\boldsymbol{\theta}, m)$. We initially propose to move to a new model, $m'$ where we choose each alternative model with equal probability. Given the proposed model we generate new parameter values $\boldsymbol{\theta}' \sim q(\boldsymbol{\theta}')$ where $q$ is some proposal distribution function described in more detail below. We accept the move with probability $\min(1, A)$, where

$$A = \frac{\pi(\boldsymbol{\theta}', m'|\boldsymbol{\upsilon})P(m|m')q(\boldsymbol{\theta})}{\pi(\boldsymbol{\theta}, m|\boldsymbol{\upsilon})P(m'|m)q(\boldsymbol{\theta}')} \left|\frac{d\boldsymbol{\theta}'}{d\boldsymbol{\theta}}\right|.$$

We note that the probabilities of moving from model $m$ to model $m'$, expressed as $P(m'|m)$ and from model $m'$ to model $m$, expressed as $P(m|m')$, are equal ($= \frac{1}{7}$) and cancel in the acceptance probability. The final Jacobian term, $\left|\frac{d\boldsymbol{\theta}'}{d\boldsymbol{\theta}}\right|$, is simply equal to unity, so that the acceptance probability term $A$, reduces to,

$$A = \frac{\pi(\boldsymbol{\theta}', m'|\boldsymbol{\upsilon})q(\boldsymbol{\theta})}{\pi(\boldsymbol{\theta}, m|\boldsymbol{\upsilon})q(\boldsymbol{\theta}')}.$$

The final quantity to be defined in the updating step is the proposal density $q$. For this study, the proposal density $q$ is a multivariate normal density function with mean (SD) and covariance matrix obtained from an initial pilot MCMC simulation for the given model. For further discussion of the MCMC reversible jump algorithm in ecological contexts see for example, King *et al.* (2009).

# 3. Results

## 3.1. Bayesian Analysis

We specify independent priors on each of the parameters. Without any prior information we set $\beta_1 \sim U[0, 1]$ and $\beta_2 \sim U[0, 1]$ and specify a hierarchical prior (Gelman 2006; Gustafson

*et al.* 2006) on the interaction parameters. In particular, we set $\log \gamma \sim N(0, \sigma^2)$ for $\gamma = \gamma_{11}, \gamma_{12}, \gamma_{22}$ where $\sigma \sim U[0, 10]$.

We initially present the results for each individual model, before considering the issue of model selection. In each model the MCMC algorithm is run for $10,000$ iterations with the first 1000 iterations discarded as burn-in. Running independent simulations from over-dispersed starting points produced essentially identical results and standard convergence diagnostics such as the BGR statistic (Brooks and Gelman 1998) suggested the chains had converged. The posterior summary statistics of the parameters in each individual model are given in Table 1. The results also indicate that the intraspecific interaction for both species is relatively lower than that of the interspecific interaction. For example, in the saturated model, model 8, the posterior mean (SD) for the interspecific interaction is 0.028 (0.029) whereas that for the intraspecific interaction parameters are 0.591 (0.224) and 0.405 (0.182).

Overall, the posterior estimates obtained indicate that there is a negative relationship between the intensity parameters and the interaction parameters. This is to be expected, since smaller values of the interaction parameters correspond to increased inhibitions (either between or within species) which will typically result in an increased intensity to explain the observed point pattern and number of observed points (and vice versa). This negative correlation is clearly demonstrated in the posterior correlation between the intensity and associated interaction parameters. For example, in the saturated model, the posterior correlation between intensity and intraspecific interaction in species 1 is $-0.561$ in the case of species 2, the posterior correlation is $-0.471$.

[Table 1 about here.]

We now consider the issue of model selection. The corresponding posterior model probabilities are also provided in Table 1. The model with the highest posterior probability corresponds to model 5, which contains one interaction parameter ($\gamma_{12}$): the interaction between the two species. We note however that models 6 and 7 received similar posterior support (0.099, and 0.094). All models identified with non-negligible support contain the between species interaction parameter, $\gamma_{12}$ indicating that the parameter and hence the interaction are important. The corresponding posterior probabilities for the presence of $\gamma_{11}$ and $\gamma_{22}$ are similar, being equal to 0.117 and 0.112 or, equivalently, Bayes Factors (Kass and Raftery 1995) of 0.132 and 0.126, respectively (assuming all interactions are present) indicating a lack of posterior support for each within-species interaction.

In the saturated model, the posterior probability that $\gamma_{12}$ is less than $\gamma_{11}$ is 1; similarly, the posterior probability that $\gamma_{12}$ is less than $\gamma_{22}$ is 1. Recall that lower values of the interaction parameter corresponds to a greater level of inhibition. This demonstrates the importance of the between species interaction within the model, and hence a high posterior model probability of being present. In the case of the intraspecific interaction estimates, the probability that $\gamma_{11}$ is greater than $\gamma_{22}$ is 0.260, suggesting the level of within-species inhibition in species 2 is higher than that of species 1.

[Table 2 about here.]

We now consider the issue of prior sensitivity of the model parameters on the posterior model probabilities (the model parameters were insensitive to vague prior specifications). We used

a hierarchical prior on the variance of the interaction terms, $\sigma^2$, and set $\sigma \sim U[0, 10]$. Note that the estimation of this parameter is expected to be poor due to the very limited amount of information relating to this parameter. In addition, this parameter, $\sigma$, is present in all models except for model 1 (corresponding to the Poisson process). Thus, we would anticipate that changing the upper limit of the uniform prior would have limited impact on the posterior model probabilities within those models that contain an interaction (models 2-8). We consider the priors $\sigma \sim U[0, 1]$ and $\sigma \sim U[0, 100]$, with the corresponding posterior model probabilities obtained given in Table 2.

In our case, increasing the upper limit of the uniform prior on $\sigma^2$ does not result in any significant changes in the posterior model probabilities. Placing a much lower value for the upper limit does have some impact on the posterior model probabilities, in the case that the limit begins to influence the posterior distribution for $\sigma$ by constraining the values the parameter can take. For example, specifying a $U[0, 1]$ prior on $\sigma$ results in a more constrained distribution for $\gamma_{12}$. However, this prior would not be regarded as uninformative as it strongly influences the set of values the parameter can take due to its restrictive nature.

### 3.2. Interaction radius sensitivity

The interaction radii (or 'zones of influence') used for the species in this analysis are based on the ranges suggested by (Illian *et al.* 2009). The range for the interaction radius for *B. attenuata* is $1.5 - 4.0$ m and that for *B. menziesii* is $0.5 - 2.5$ m. We adopt an interaction radius sensitivity analysis using the same priors and interaction function described earlier. The additional interaction radii considered are 1.0, and 3.5 (recall previously that a radius of 2.5m was used). Figure 4 shows the reduced dataset (bivariate point pattern) after border edge correction has been applied for each of the radii considered.

[Figure 4 about here.]

The results of the interaction radius sensitivity test are shown in Figure 3. The results indicate that as the interaction radius is increased, the posterior estimates for the interaction parameters increase in magnitude suggesting a decrease in the degree of inhibition between plants concerned. This is especially true for the intraspecific interaction parameters. Finally, the effect of the choice of interaction radius on model discrimination was also considered. The results indicate that the choice of interaction does affect the model which receives the highest posterior support. The posterior probabilities for the interspecific interaction parameter for radii 1.0, 2.5 and 3.5 are 0.040, 1.000, and 0.605 respectively.

[Table 3 about here.]

[Table 4 about here.]

## 4. Discussion

The analysis of bivariate (or multivariate) spatial point patterns of species can lead to an understanding of the interactions involved within and among different types (or species) of

individuals forming the patterns. We have considered a Bayesian approach to analysing bivariate point patterns, with particular focus on model choice, i.e. on the assessment of the presence/absence of interactions present within the pattern. In particular, we obtain posterior model probabilities for the different competing models that quantitatively discriminate among the competing models and hence interactions present using a pilot-tuned reversible jump MCMC algorithm.

Biologically, the interactions are interpreted as competitive interactions where the magnitude of the interaction gives an indication of the 'competitive strength'. In this analysis, we are able to not only quantify the presence/absence of the parameters for models where there is more than one interaction present, but also to obtain the relative strength of the interactions, by calculating the posterior probability that one interaction is greater than another. For our dataset, the intraspecific inhibitory interactions occurring in both resprouter species were found to be of similar strength. For the interaction between the two species there was strong evidence of the parameter representing this interaction should be included in the model.

Both species considered in this analysis are of the same genus, *Banksia* and hence possess similar biological characteristics. This is a possible explanation for the fact that the posterior estimates of the intraspecific interaction parameters were of similar magnitude. The posterior mean (SD) of the intraspecific interaction parameters for species 1 and 2 are 0.591 (0.224) and 0.405 (0.182), respectively, indicating that there is no evidence for a decisive characterisation of the nature of the intraspecific interaction. This is corroborated by the results of the exploratory analysis. With regard to the inter-specific interaction between the species, Richardson *et al.* (1995) describe the interaction between *Banksia* species as most strongly competitive (in comparison with the interaction between individuals of the *Banksia* species and other species) due to the fact that individuals of *Banksia* possess common features such as similar growth form and germination biology. Again, this is also evident in the results obtained. The value of the posterior estimate for the interspecific interaction parameter is comparatively much lower than that of the other interaction parameters. Individuals of two species exhibit proteoid or cluster roots, a feature common to all species of the genus *Banksia*. This root system involves masses of lateral roots giving rise to a dense horizontal root mat system. The inhibitory interaction between the two species could be due to competition between the species at the level of nutrient uptake by the root system. Connor and Bowers (1987) suggest that inter-specific competition gives rise to spatial signatures inherent in spatial point patterns.

Possible extensions to this approach in general include the use of covariates in the model, the consideration of asymmetric interactions between species and the use of area interaction point processes (Baddeley and Lieshout 1995; Comas and Mateu 2007). The inclusion of environmental covariates in the modelling process would lead to more complex point processes. Finally, the extension to multivariate point processes with more than two species is an area of active research where we consider novel approaches to circumventing the huge computational costs to modelling a highly diverse ecological communities.

## References

Armstrong P (1991). "Species Patterning in the Heath Vegetation of the Northern Sandplain." *Honours thesis, University of Western Australia.*

Baddeley A, Bárány I, Schneider R (2007). "Spatial Point Processes and their Applications." In *Stochastic Geometry*, volume 1892 of *Lecture Notes in Mathematics*, pp. 1–75. Springer Berlin / Heidelberg.

Baddeley A, Lieshout M (1995). "Area Interaction Point Processes." *Annals of the Institute of Statistical Mathematics*, **47**, 601–619.

Baddeley A, Turner R (2000). "Practical Maximum Pseudolikelihood for Spatial Point Patterns." *Australian and New Zealand Journal of Statistics*, **42**, 283–322.

Bell DT (2001). "Ecological Response Syndrome in the Flora of Southwestern Western Australia: Fire Resprouters versus Reseeders." *The Botanical Review*, **67**.

Berthelsen KK, Møller J (2002). "A primer on perfect simulation for spatial point processes." *Bulletin Brazilian Mathematical Society*, **33**, 351–367.

Besag J (1977). "Contribution to the discussion of Dr.Ripley's paper." *Royal Statistical Society B*, **39**, 193–195.

Brooks SP (1998). "Markov Chain Monte Carlo Method and its Application." *The Statistician*, **47**, 69–100.

Brooks SP, Gelman A (1998). "General Methods for Monitoring Convergence of Iterative Convergence." *Journal of Computational and Graphical Statistics*, **7**, 434–455.

Callaway RM (1995). "Positive Interactions Among Plants." *The Botanical Review*, **61**, 306–337.

Chang IH, Mukerjee R (2006). "Probability matching property of adjusted likelihoods." *Statist. Probab. Lett.*, **76**, 838–842.

Comas C, Mateu J (2007). "Modelling Forest Dynamics: A Perspective from Point Process Methods." *Biometrical Journal*, **49**, 176 – 196.

Connor EF, Bowers MA (1987). "The Spatial Consequences of Interspecific Competition." *Annales Zoologici Fennici*, **24**.

Diggle P (2003). *Statistical Analysis of Spatial Point Patterns, Second Edition.* Oxford University Press.

Diggle PJ (1983). *Statistical analysis of spatial point patterns.* Academic Press Inc.

Efron B (1993). "Bayes and likelihood calculations from confidence intervals." *Biometrika*, **80**, 3–26.

Ewel JJ, Hiremath AJ (2006). *Plant-Plant Interactions in Tropical Forests.* Cambridge University Press.

Gatrell AC, Bailey TC, Diggle PJ, Rowlingson BS (1996). "Spatial Point Pattern Analysis of Aerial Survey Data to Assess Clustering in Wildlife Distributions." *Transactions of the Institute of British Geographers*, **21**, 256 – 274.

Gelman A (2006). "Prior Distributions for Variance Parameters in Hierarchical Models." *Bayesian Analysis*, **1**, 515 – 533.

Green PJ (1995). "Reversible Jump MCMC Computation and Bayesian Model Determination." *Biometrika*, **82**, 711–732.

Grinnell J (1917). "Field Tests of Theories Concerning Distributional Control." *The American Naturalist*, **51**, 115.

Gustafson P, Hossain S, MacNab YC (2006). "Conservative Prior Distributions for Variance Parameters in Hierarchical Models." *Canadian Journal of Statistics*, **34**, 377 – 390.

Hubbell SP (1997). "A Unified Theory of Biogeography and Relative Species Abundance and its Application to Tropical Rainforests and Coral Reefs." *Coral Reefs*, **16**, 9–21.

Illian J, Møller J, Waagepetersen RP (2009). "Hierarchical Spatial Point Process Analysis for a Plant Community with High Biodiversity." *Environmental and Ecological Statistics*, **42**, 283–322.

Illian J, Penttinen A, Stoyan H, Stoyan D (2008). *Statistical Analysis and Modelling of Spatial Point Patterns*. John Wiley and Sons, Chichester.

Illian JB, Hendrichsen DK (2010). "Gibbs Point Process Models with Mixed Effects." *Environmetrics*, **21**, 241 – 353.

Illian JB, Sørbye SH, Rue H, Hendrichsen D (2012). "Using INLA To Fit A Complex Point Process Model With Temporally Varying Effects Ű A Case Study." *Journal of Environmental Statistics*, **3**.

Janzen DH (1970). "Herbivores and the Number of Tree Species in Tropical Forests." *The American Naturalist*, pp. 104–501.

Kass RE, Raftery AE (1995). "Bayes Factors." *Journal of the American Statistical Association*, **90**, 773–795.

Khaemba WM (2001). "Spatial Point Pattern Analysis and its Application in Geographical Epidemiology." *International Journal of Applied Earth Observation and Geoinformation*, **3**, 139 – 145.

King R, Illian JB, King SE, Nightingale GF, Hendrichsen DK (2012). "A Bayesian Approach to Fitting Gibbs Processes with Temporal Random Effects." *Journal of Agricultural, Biological, and Environmental Statistics*, **17**, 601–622.

King R, Morgan BJT, Gimenez O, Brooks SP (2009). *Bayesian Statistics for Population Ecology*. Chapman and Hall/CRC.

Law R, Illian J, Burslem DFRP, Gratzer G, Gunatilleke CVS, Gunatilleke IAUN (2009). "Ecological information from spatial patterns of plants insights from point process theory." *Journal of Ecology*, **97**, 616–628.

Liebhold A, Gurevitch J (2002). "Integrating the Statistical Analysis of Spatial Data in Ecology." *Ecography*, **25**, 553–557.

Møller J, Waagepetersen RP (2003). *Statistical Inference and Simulation for Spatial Point Processes*. Chapman and Hall/CRC.

Murrell DJ, Law R (2003). "Heteromyopia and the Spatial Coexistence of Similar Competitors." *Ecology Letters*, **6**, 48–59.

Picard N, Bar-Hen A, Mortier F, Chadoeuf J (2009). "The Multi Scale Marked Area Interaction Point Processes: A Model for the Spatial Pattern of Trees." *Scandinavian Journal of Statistics*, **36**, 23–41.

Richardson DM, Cowling RM, Lamont BB, van Hensbergen HJ (1995). "Coexistence of Banksia Species in Southwestern Australia: The Role of Regional and Local Processes." *Journal of Vegetation Science*, **6**, 329 – 342.

Siepielski AM, McPeek MA (2002). "On the Evidence for Species Coexistence: A Critique of the Coexistence Program." *Oecologia*, **130**, 1–14.

Stoyan D, Penttinen A (2000). "Recent applications of point process methods in forestry statistics." *Statistical Science*, **15**, 61–78.

Thompson HR (1955). "Spatial Point Processes, with Applications to Ecology." *Biometrika*, **42**, 102 – 115.

Ventura L, Cabras S, Racugno W (2009). "Prior distributions from pseudo-likelihoods in the presence of nuisance parameters." *J. Amer. Statist. Assoc.*, **104**, 768–774.

Wiegand T, Gunatilleke S, Guantilleke N (2007). "Species Associations in a Heterogeneous Sri Lankan Dipterocarp Forest." *The American Naturalist*, **170**, E77–E95.

Wiegand T, Moloney KA (2004). "Rings, Circles, and Null Models for Point Pattern Analysis in Ecology." *Oikos*, **104**, 209–229.

Wright S (2002). "Plant Diversity in Tropical Forests: a Review of Mechanisms of Species Coexistence." *Oecologia*, **130**, 1–14.

Zillio T, Condit RS (2007). "The Impact of Neutrality, Niche Differentiation and Species Input on Diversity and Abundance Distributions." *Oikos*, **116**, 931–940.

## Affiliation:

Glenna F. Nightingale
Department of Geography and Geosciences, University of St Andrews
St Andrews, Scotland
E-mail: glenna.evans@gmail.com

Journal of Environmental Statistics http://www.jenvstat.org
Volume 7, Issue 3 Submitted: 2015-01-25
September 2015 Accepted: 2015-09-01

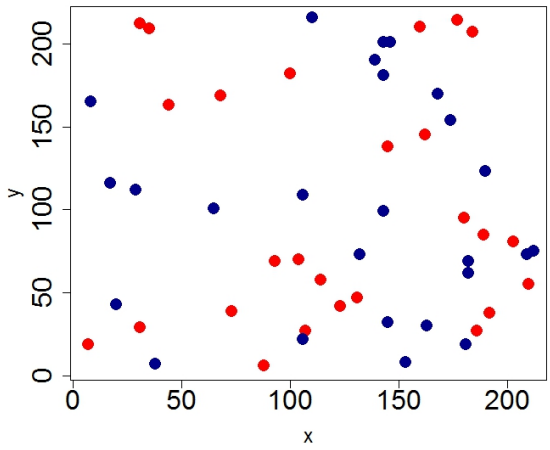


Figure 1: Plot showing the point pattern for both species considered in this analysis. *Banksia menziesii* is denoted in dark-blue font and *Banksia attenuata* in red font.

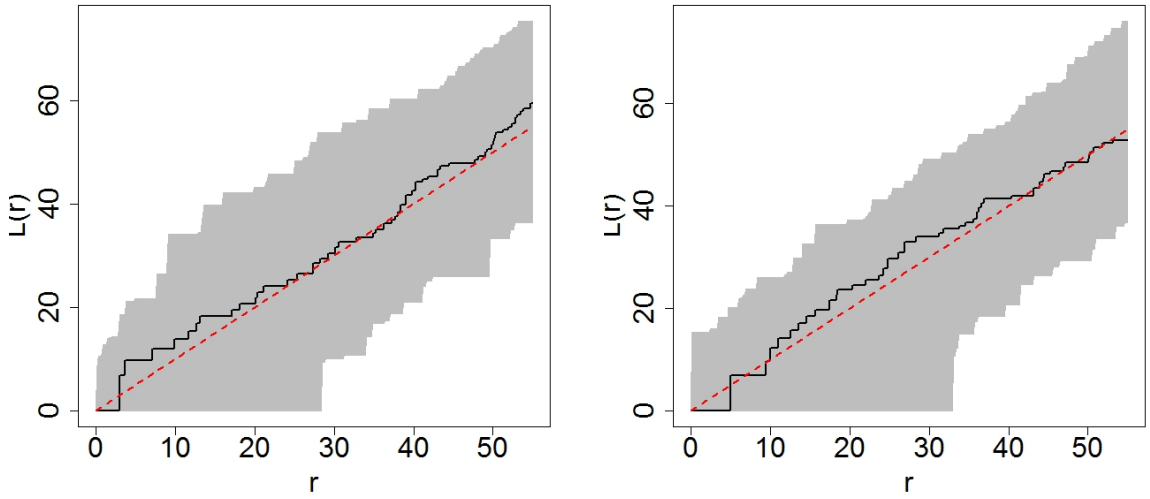


(a) (b)

Figure 2: Illustration of (a) a plot of the L-function for (*Banksia attenuata*), and (b) a plot of the L-function for *Banksia menziesii*. In both cases a simulation envelope is included representing 10,000 simulations of a point pattern with complete spatial randomness (CSR). The dark line on the plot represents the observed value of L($r$) for the data, the red line represents that for the data simulated under CSR, and the grey zone represents the upper and lower pointwise envelopes for L($r$) for the 10,000 simulated point patterns.

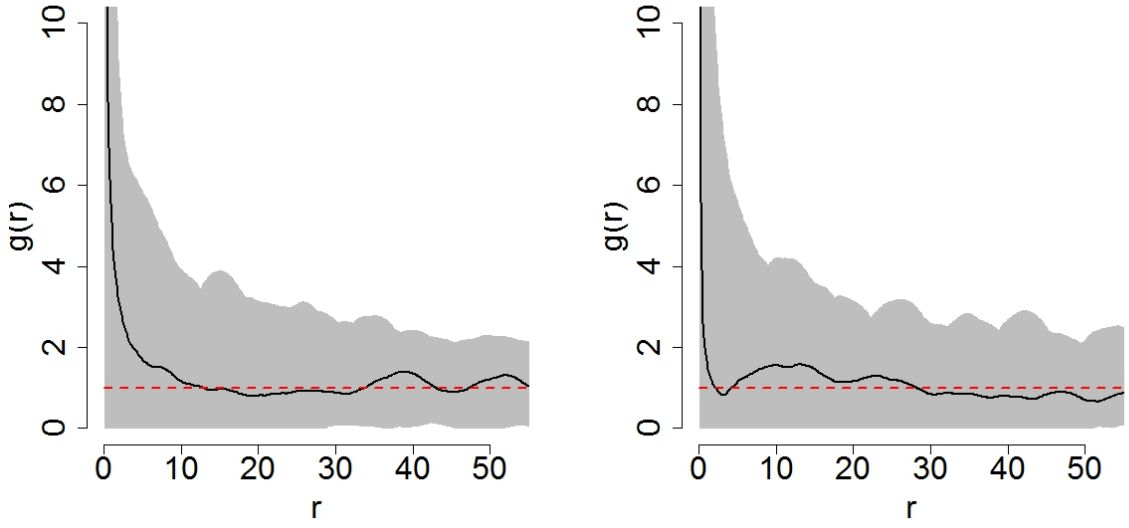


(a) (b)

Figure 3: Illustration of (a) a plot of the Pair correlation function for (*Banksia attenuata*), and (b) a plot of the Pair correlation function for *Banksia menziesii*. In both cases a simulation envelope is included representing 10,000 simulations of a point pattern with complete spatial randomness (CSR). The dark line on the plot represents the observed value of g($r$) for the data, the red line represents that for the data simulated under CSR, and the grey zone represents the upper and lower pointwise envelopes for g($r$) for the 10,000 simulated point patterns.

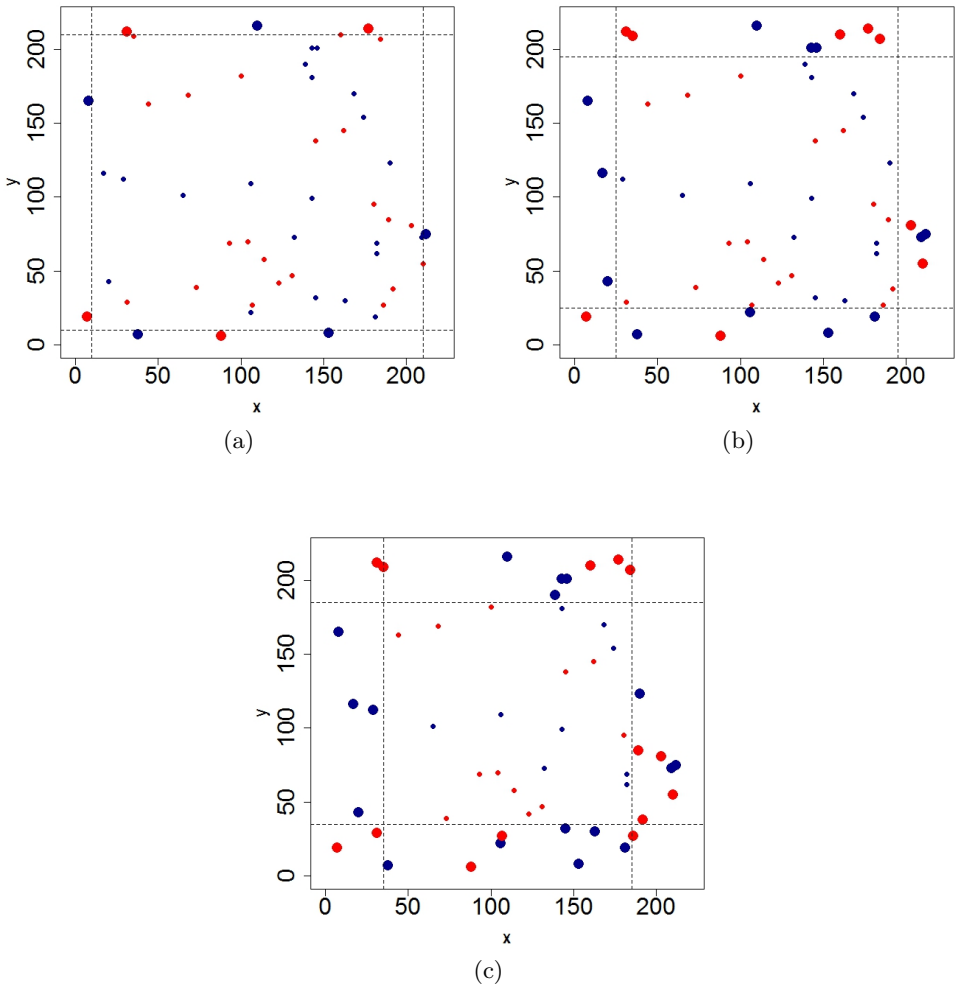


Figure 4: Plots showing the point pattern for both species considered in this analysis and the boundaries for the reduced dataset generated after applying border edge correction for an interaction radius of (a) 1.0m, (b) 2.5m, and (c) 3.5m. The original point pattern is plotted with dotted lines demarcating the boundaries for the reduced dataset for each radius. The larger points represent those that lie in the boundary area and are not included in the reduced dataset, $W_R$. *Banksia menziesii* is denoted in dark-blue font and *Banksia attenuata* in red font.

Table 1: Posterior means and 95 credible estimates for parameters ($\sigma \sim U[0, 10]$), but providing the lower and upper 2.5 quantiles. The corresponding model posterior probabilities are included in the last row of the table.

| | summary | model 1 | model 2 | model 3 | model 4 | model 5 | model 6 | model 7 | model 8 |
|---|---|---|---|---|---|---|---|---|---|
| $\beta_1$ | mean | 0.00092 | 0.00109 | 0.00094 | 0.00105 | 0.00154 | 0.00191 | 0.00155 | 0.00193 |
| | 2.5% | 0.00064 | 0.00074 | 0.00065 | 0.00072 | 0.00112 | 0.00129 | 0.00107 | 0.00132 |
| | 97.5% | 0.00123 | 0.00151 | 0.00126 | 0.00143 | 0.00198 | 0.00182 | 0.00204 | 0.00285 |
| $\beta_2$ | mean | 0.00094 | 0.00094 | 0.00104 | 0.00109 | 0.00153 | 0.00155 | 0.00212 | 0.00209 |
| | 2.5% | 0.00065 | 0.00068 | 0.00072 | 0.00071 | 0.00107 | 0.00106 | 0.00138 | 0.00137 |
| | 97.5% | 0.00127 | 0.00124 | 0.00144 | 0.00159 | 0.00205 | 0.0021 | 0.00303 | 0.00291 |
| $\gamma_{11}$ | mean | | 0.65656 | | 0.69065 | | 0.52577 | | 0.59067 |
| | 2.5% | | 0.29132 | | 0.36314 | | 0.23601 | | 0.21043 |
| | 97.5% | | 0.95715 | | 0.97398 | | 0.88642 | | 0.94222 |
| $\gamma_{22}$ | mean | | | 0.67496 | 0.64488 | | | 0.39273 | 0.40465 |
| | 2.5% | | | 0.30095 | 0.25179 | | | 0.13141 | 0.15673 |
| | 97.5% | | | 0.98722 | 0.97269 | | | 0.82675 | 0.77501 |
| $\gamma_{12}$ | mean | | | | | 0.02872 | 0.02935 | 0.02628 | 0.02802 |
| | 2.5% | | | | | 0.00285 | 0.00301 | 0.00277 | 0.00224 |
| | 97.5% | | | | | 0.08559 | 0.08882 | 0.07841 | 0.09033 |
| $\sigma$ | mean | | 2.76207 | 2.77485 | 1.53353 | 5.73799 | 4.66448 | 4.85169 | 3.9134 |
| | 2.5% | | 0.15489 | 0.04969 | 0.13592 | 2.16859 | 1.69462 | 1.78708 | 1.46741 |
| | 97.5% | | 8.36174 | 8.49629 | 5.52905 | 9.46288 | 9.00272 | 9.13801 | 8.11552 |
| Model posterior Pr | | 0.000 | 0.000 | 0.000 | 0.000 | 0.789 | 0.099 | 0.094 | 0.018 |

Table 2: Posterior model probabilities for prior sensitivity analysis ($\sigma \sim U[0,1]$, and $\sigma \sim U[0,100]$).

| Model | $U[0,1]$ | $U[0,100]$ |
|---|---|---|
| 1 | 0.012 | 0.003 |
| 2 | 0.003 | 0.000 |
| 3 | 0.002 | 0.000 |
| 4 | 0.017 | 0.000 |
| 5 | 0.448 | 0.846 |
| 6 | 0.199 | 0.069 |
| 7 | 0.208 | 0.071 |
| 8 | 0.112 | 0.011 |

Table 3: Posterior means and 95 credible estimates for parameters ($\sigma \sim U[0, 10]$), but providing the lower and upper 2.5 quantiles. The heading for each column in the table indicates the radius in meters used.

| parameter | summary | 1.0 | 2.5 | 3.5 |
|---|---|---|---|---|
| $\beta_1$ | mean | 0.0003 | 0.00193 | 0.001 |
| | 2.5% | 0.00015 | 0.00132 | 0.0008 |
| | 97.5% | 0.0007 | 0.00029 | 0.003 |
| $\beta_2$ | mean | 0.0002 | 0.0021 | 0.0037 |
| | 2.5% | 0.00013 | 0.00137 | 0.0004 |
| | 97.5% | 0.0006 | 0.00029 | 0.0009 |
| $\gamma_{11}$ | mean | 0.041 | 0.591 | 0.269 |
| | 2.5% | 0.0012 | 0.210 | 0.111 |
| | 97.5% | 0.985 | 0.942 | 0.949 |
| $\gamma_{22}$ | mean | 0.133 | 0.405 | 0.126 |
| | 2.5% | 0.0092 | 0.157 | 0.044 |
| | 97.5% | 0.991 | 0.755 | 0.939 |
| $\gamma_{12}$ | mean | 0.219 | 0.028 | 0.126 |
| | 2.5% | 0.026 | 0.002 | 0.044 |
| | 97.5% | 0.991 | 0.09 | 0.939 |
| $\sigma$ | mean | 1.37 | 3.91 | 2.25 |
| | 2.5% | 0.052 | 1.29 | 0.637 |
| | 97.5% | 5.81 | 8.92 | 6.83 |

Table 4: Posterior model probabilities for interaction sensitivity analysis ($r = 1.0m$, $r = 2.5m$, and $r = 3.5m$) where $\sigma \sim U[0, 10]$.

| Model | $1.0m$ | $2.5m$ | $3.5m$ |
|---|---|---|---|
| 1 | 0.749 | 0 | 0.375 |
| 2 | 0.097 | 0 | 0.003 |
| 3 | 0.051 | 0 | 0.008 |
| 4 | 0.062 | 0 | 0.007 |
| 5 | 0.010 | 0.789 | 0.221 |
| 6 | 0.013 | 0.099 | 0.063 |
| 7 | 0.011 | 0.094 | 0.224 |
| 8 | 0.0064 | 0.018 | 0.097 |